first three elements of $z_{i,j+1}$ can be obtained from Eq. (8). The fourth element at $j + 1$ can be computed explicitly at each i from the fourth row of Eq. (2) using the first three elements of $z_{i,j+1}$. Since all of the 4×4 matrices in Eq. (8) are independent of j they should be stored.

The number of multiplications and divisions initially required to compute $(\delta^2/2\Delta)A_i$, $(\delta^2/2\Delta)B_i$, and $(\delta^2/2\Delta)C_i$ is essentially the same as with the Houbolt scheme. The number of operations required for the first three elements of $z_{i,j+1}$ is 1) $\delta^2/2\Delta g_{i,j} = 3$, 2) $[2D + \delta^2/2\Delta B_i]z_{i,j} = 12$, 3) $\delta^2/2\Delta A_i z_{i+1,j} = 12$, and 4) $\delta^2/2\Delta\ C_i z_{i-1,j} = 12$. The fourth element requires 10, for a total of 49 per station per time step. If account is taken of the fact that there are several zeros in A_i,B_i, and C_i, the total reduces to 44. For a cylindrical shell of uniform thickness there are many zeros in the matrices and it is more efficient to treat each multiplication individually rather than to use the general matrix multiplication procedures indicated in Eq. (8). For this case, the total reduces to 34 operations per station per time step.

Nonlinear Problems

The author has used the Houbolt scheme defined by Eq. (5) to compute the geometrically nonlinear response of arbitrarily loaded shells.[3] The nonlinearities are treated as pseudo loads and are incorporated with the load vector $g_{i,j}$. Several iterations are allowed at each time step if the latest estimated solution at j and the computed solution at j differ by more than a prescribed amount. Thus, $(60 + T)\beta$ multiplications and divisions occur at each time step where β is the number of iterations and T is the computation of the nonlinearities. If a sufficiently small time step is used, no iterations are necessary and $\beta = 1$. An alternative procedure is to include the nonlinearities in $g_{i,j}$, but use the explicit scheme defined by Eq. (8). For this case, $44 + T$ multiplications and divisions are required at each time step.

Conclusions

The Houbolt scheme requires an initial expenditure of approximately 250 multiplication and divisions per station to compute the matrices A_i,$\bar{B}_i$ and C_i plus 285 per station to compute the recursive matrices P_i,Q_i, and R_i. The transient solution requires 60 operations per station per time step. The explicit scheme requires an initial expenditure of approximately 250 operations per station to compute the A_i,B_i, and C_i matrices, and the solution takes 44 operations per station per time step for the general shell. Thus, the explicit scheme should be approximately 35% faster than the Houbolt scheme per time step.

For a uniform cylinder, the explicit scheme operations reduce to 34, and hence it should be approximately 75% faster. This conclusion is not supported by the evidence presented in Ref. 1. However, the computer times given in Ref. 1 were for an explicit method that used three variables instead of four. Communication with the senior author of Ref. 1 revealed that the details of the program based on the three variables u,v, and w differ somewhat from the four variable explicit procedure presented in Sec. 5 of Ref. 1 and in this Note. For example, the equations of motion contained the spatial derivatives instead of the differences as in Eq. (2), and the derivatives u',u'',v',v'',w',w'', and w^{iv} were efficiently computed by addition and subtraction, i.e. $\Delta^2 u'' = u_{i+1} - u_i - u_i + u_{i-1}$, rather than multiplication. Using these and similar techniques, the number of required multiplications and divisions can be reduced to 15 per station per time step, excluding the effort required to generate the load terms. Thus, the ratio between the Houbolt scheme and the three variable explicit scheme used by the authors of Ref. 1 is 60/15, which is much closer to the speed ratio of 6 reported in Ref. 1. More computer time was required when the four variable method was used. The senior author of Ref. 1 estimates that approximately 30 multiplications and divisions are required when the same techniques are applied to the general shell of revolution. Thus, this other explicit scheme should be approximately 50% faster than the explicit scheme described here.

For nonlinear response, the Houbolt scheme requires $(60 + T)\beta$ multiplications and divisions, and the explicit scheme described in this note takes $44 + T$. Thus, this explicit scheme should be less than $35\beta\%$ faster than the Houbolt scheme. If the time step is small enough, $\beta = 1$.

There are several other features to consider when selecting an integration scheme, such as numerical instability and numerical damping. The Houbolt scheme is numerically stable; the explicit scheme is not. The Houbolt scheme introduces significant damping if δ becomes too large; the explicit scheme does not. Because of stability considerations a larger time increment can be used in the Houbolt scheme than in the explicit scheme, and consequently when the solution varies slowly, the Houbolt scheme can require less computation time over the total response period.

References

[1] Johnson, D. E. and Grief, R., "Dynamic Response of a Cylindrical Shell: Two Numerical Methods," *AIAA Journal*, Vol. 4, No. 3, March 1966, pp. 486–494.

[2] Crandall, S., *Engineering Analysis, A Survey of Numerical Procedures*, McGraw-Hill, New York, 1956, pp. 34–35.

[3] Ball, R. E., "A Program for the Nonlinear Static and Dynamic Analysis of Arbitrarily Loaded Shells of Revolution," Presented at the Computer-oriented Analysis of Shell Structures Conference, Palo Alto, Calif., Aug. 1970, *Journal of Computers and Structures*, to be published.

[4] Stephens, W. B. and Robinson, M. P., "Computer Program for Finite-difference Solutions of Shells of Revolution Under Asymmetric Dynamic Loading," TN D-6059, Jan. 1971, NASA.

[5] Houbolt, J. C., "A Recurrence Matrix Solution for the Dynamic Response of Aircraft in Gusts," Rept. 1010, 1951, NACA.

[6] Budiansky, B. and Radkowski, P., "Numerical Analysis of Unsymmetrical Bending of Shells of Revolution," *AIAA Journal*, Vol. 1, No. 8, Aug. 1963, pp. 1833–1842.

Maximal Plastic Deformation of Semi-Infinite Rods

W. C. SWEATT* AND W. J. STRONGE†
Naval Weapons Center, China Lake, Calif.

THE dynamic response of structures deformed beyond the elastic limit is a function of both the magnitude and the history of the applied load $p(t)$. With any loading system, whether it is a punch press or a blast wave, there are certain constraints for example, on the available energy or the maximum pressure that can be applied. When the loading can be controlled within these constraints, it is an optimization problem to determine the $p(t)$ that results in the maximum plastic deformation. This Note examines a simple problem which shows that two common assumptions, that the loading system either applies a certain impulse or imparts a certain energy to the structure, result in distinctly different optimal load histories.

We consider a case of elasto-plastic wave propagation in a semi-infinite rod. The rod is composed of a linearly work-

Received March 22, 1971.
Index categories: Structural Dynamic Analysis; Launch Vehicle and Missile Fabrication.

* Mechanical Engineer.
† Mechanical Engineer. Member AIAA.

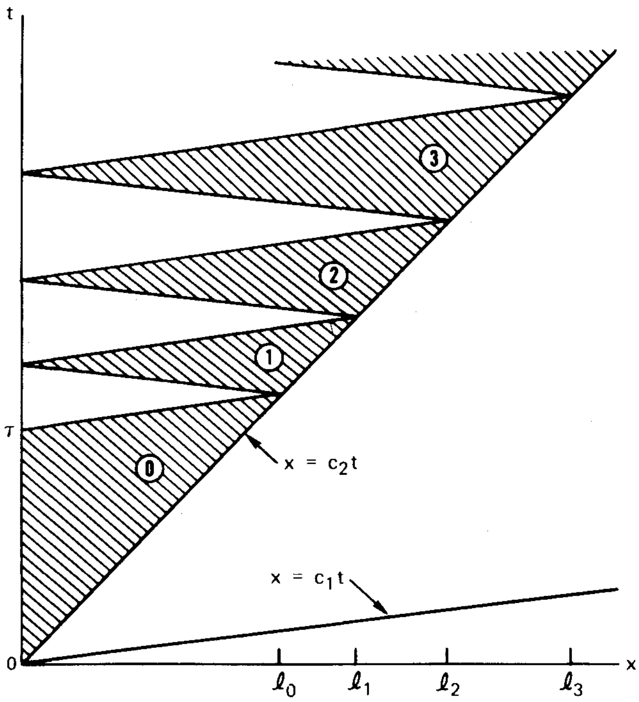

Fig. 1 Regions of constant stress in the characteristic field.

hardening material where the elastic and plastic moduli, denoted by E_1 and E_2, respectively, are separated by an initial yield stress σ_y. A pressure in excess of σ_y is applied to the end of the rod for a limited period of time. In this analysis the class of admissible pressures has been restricted to rectangular functions of time; i.e., suddenly applied, held constant, and then suddenly released. We wish to determine the $p(t)$, within this class of loads, that maximizes the permanent displacement of the end of the rod.

Analysis

A solution for the stress field in the rod can be obtained by the method of characteristics.[1,2] This solution has a two-wave character; the elastic and plastic wave speeds are denoted by c_1 and c_2, respectively, where $c_i^2 = E_i/\rho$. The characteristic field associated with this problem is shown in Fig. 1. The stress is constant throughout each region on this figure. In the numbered regions, where plastic deformation has occurred, the stress is

$$\sigma_m = P[(\alpha - 1)/(\alpha + 1)]^m \tag{1}$$

where m is the number designating a region, P is the force per unit area applied to the end of the rod and $\alpha = c_1/c_2$. Note that a pressure, resulting in a compressive stress wave, is associated with a negative value of P. The plastic part of the strain will be

$$\epsilon_m{}^p = (\sigma_m - \sigma_y)(E_1 - E_2)/E_1E_2 \tag{2}$$

Here, σ_y is considered to have the same sign as P. The length l_m of each numbered region of constant stress will be

$$l_m = (c_1\tau/\alpha - 1)(\alpha + 1)^m/(\alpha - 1)^m \tag{3}$$

where τ is the duration of the applied pressure. At time τ the pressure is suddenly removed from the end of the rod.

The regions where plastic deformation has occurred continue, with the stress level decreasing successively, until the stress is no longer greater than σ_y. The last of these regions, denoted by M, can be determined from

$$[(\alpha - 1)/(\alpha + 1)]^{M+1} \leqq \sigma_y/P \tag{4}$$

Here, M is the smallest integer that satisfies this relation. In the case of equality, $\sigma_{M+1} = \sigma_y$ whereas inequality implies $|\sigma_{M+1}| < |\sigma_y|$.[3]

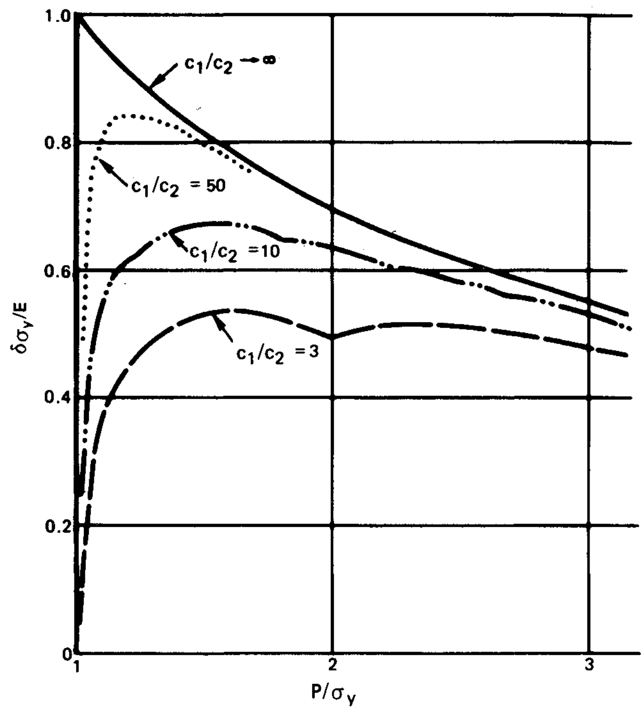

Fig. 3 Ratio of final displacement of end of the rod to energy imparted.

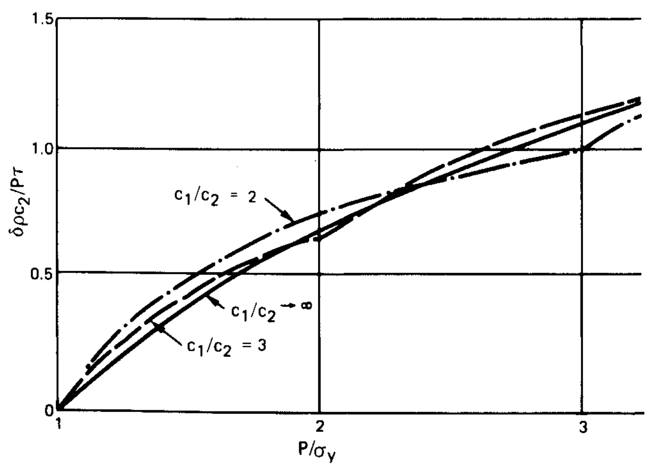

Fig. 2 Ratio of final displacement of end of the rod to impulse applied.

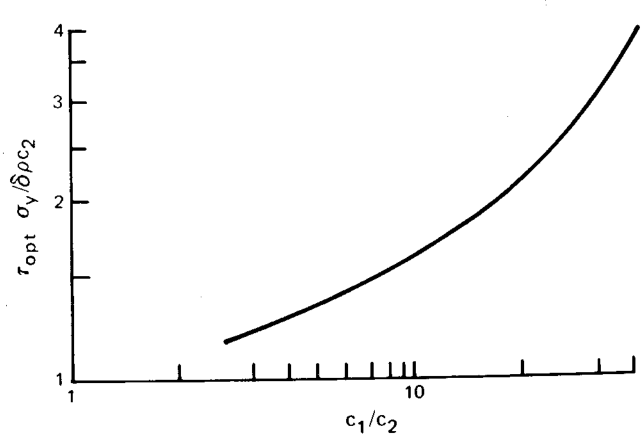

Fig. 4 Optimal load duration with energy constraint.

Impulse Constraint

The deformation associated with plastic strain occurs across the c_2 characteristic wave front. This plastic deformation within the bar results in a displacement δ of the end of the rod‡

$$\delta = \sum_{m=0}^{M} \epsilon_m{}^P[l_m - l_{m-1}] \tag{5}$$

where, by definition, δ is positive when the rod is lengthened and $l_{-1} = 0$. Substituting into Eq. (5) from Eqs. (1–4) we obtain a nondimensional ratio of displacement to impulse applied at the end of the rod

$$\delta \rho c_2/P\tau = [(\alpha + 1)/\alpha]\{1 + 2M/(\alpha + 1) - (\sigma_y/P)[(\alpha + 1)/(\alpha - 1)]^M\} \tag{6}$$

This ratio of displacement to impulse is shown in Fig. 2.

With this idealized material, the impulse response curves are not very sensitive to changes in α. The family of curves is closely approximated by

$$\delta \rho c_2/P\tau = \ln(P/\sigma_y) \tag{7}$$

with the variation about this function increasing as α decreases.§ The impulse response curves show an increasing ratio of displacement to impulse with increasing P/σ_y. Consequently, for this class of loads, an impulsive pressure (Dirac delta function) results in the maximum displacement from any given impulse.

Energy Constraint

The energy per unit area, denoted by E, that is imparted to the bar will be

$$E = \int_0^\infty p(t)v(0,t)dt \tag{8}$$

where $v(0,t)$ is the particle velocity at the end of the rod. Since $p(t)$ is a constant during $[0,\tau]$ and then vanishes

$$E = (P\tau/\rho c_1)[P\alpha - \sigma_y(\alpha - 1)] \tag{9}$$

This equation, together with Eq. (6), results in a nondimensional ratio of displacement to energy

$$\delta\sigma_y/E = \{(\alpha + 1)\sigma_y/P/[\alpha - (\alpha - 1)\sigma_y/P]\}\ \{1 + 2M/(\alpha + 1) - (\sigma_y/P)[(\alpha + 1)/(\alpha - 1)]^M\} \tag{10}$$

that is shown in Fig. 3. From these curves, the value of P that will maximize the displacement-energy ratio can be determined. A corresponding load duration for maximal deformation, τ_{opt}, is shown in Fig. 4. In contrast to the case where impulse was limited, the optimal value depends on α.

Conclusion

Results have been obtained for a system that represents some metal forming operations where either the impulse or the energy imparted to the system on each stroke is limited. The results for the cases of an impulse constraint and an energy constraint are distinct. With a constraint on impulse, the deformation is maximized by applying the greatest pressure in the shortest possible time. With a constraint on energy, a longer time results in the maximal deformation; the corresponding applied pressure is not much larger than the yield stress. In general, these results indicate that if one wishes to obtain maximal deformations from some loading system, the constraints peculiar to that system must be identified.

‡ If the pressure is either increased or decreased slightly during the loading period, this displacement magnitude is only changed slightly.

§ The limiting case, $\alpha \to \infty$, results from either the rigid-strain hardening or the elastic-perfectly plastic material descriptions. In the first case, $E_1 \to \infty$ and the plastic deformation is confined to the length l_0. In the second case, $E_2 = 0$ and the plastic deformation is limited to the end of the rod. The latter is necessarily a large deformation result.

References

[1] Hopkins, H. G., "The Method of Characteristics and its Application to the Theory of Stress Waves in Solids," *Engineering Plasticity*, edited by J. Heyman and F. A. Leckie, Cambridge University Press, 1968, pp. 277–315.

[2] Lee, E. H. and Tupper, S. J., "Analysis of Plastic Deformation in a Steel Cylinder Striking a Rigid Target," *Journal of Applied Mechanics*, Vol. 21, 1954, pp. 63–70.

[3] Cristescu, N., *Dynamic Plasticity*, North-Holland, Amsterdam, 1967, pp. 63–65.

Discretization and Computational Errors in High-Order Finite Elements

Isaac Fried*
Massachusetts Institute of Technology, Cambridge, Mass.

1. Introduction

DISCRETIZATION of an elliptic equation of the $2m$th order ($m = 1$ harmonic, $m = 2$ biharmonic) by finite elements of diameter h, inside which the interpolation polynomials include a complete set of degree p, assures[1] that the error in the energy is decreased as $h^{2(p+1-m)}$. Thus, by reducing the mesh size h sufficiently, one theoretically should be able to obtain any desired accuracy in the solution. Unfortunately, roundoff errors coupled with the particular nature of the difference matrices generated by the finite element method drastically alter this prediction.

The roundoff errors affecting the accuracy of x in solving the linear system $Kx = b$ come from two sources: from truncating or rounding the initial data in K and b, and from the accumulation of errors during the solution process. It has been shown[2–3] that with current methods of solution these two sources give rise to errors of similar magnitude. In the case where the data is given exactly, the solution can be improved iteratively.[4] But since in practice the data is never given exactly, it is the most serious source of error. Basically, this error is a function of the accuracy of the computer and of the condition of the global (stiffness) matrix K.

The difference matrices generated by either the finite element or finite difference method inevitably become ill-conditioned as the mesh of elements is refined. In fact, the spectral condition number of K, $Cn(K)$, increases as ch^{-2m}, where c is a function of various mesh parameters. Hence as the mesh is refined the discretization errors decrease, but simultaneously the effect of roundoff errors increases until at a certain h they become dominant. In this respect the higher order (say bending where $m = 2$) problems are more prone to round off error perturbation than the lower order ones. Now since p, the order of the element, appears in the exponent of h in the expression for the discretization errors but not in the expression for the condition number, by using higher order elements one expects to reduce the relative effect of roundoff

Received March 24, 1971; revision received June 7, 1971. This research was supported in part by the Office of Scientific Research of the USAF under Contract F44620-67-C0019. The author wishes to express his appreciation to T. H. H. Pian for his support.

Index category: Structural Static Analysis.

* Post Doctoral Research Fellow, Department of Aeronautics and Astronautics.